Photoacoustics 30 (2023) 100478

Contents lists available at ScienceDirect

Photoacoustics

journal homepage: www.elsevier.com/locate/pacs

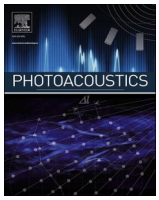

Fano meets Stokes: Four-order-of-magnitude enhancement of asymmetric Brillouin light scattering spectra

Rafał Białek [a,*], Thomas Vasileiadis [a], Mikołaj Pochylski [a], Bartłomiej Graczykowski [a,b,**]

[a] Faculty of Physics, Adam Mickiewicz University, Poznań, ul. Uniwersytetu Poznańskiego 2, 61-614 Poznań, Poland
[b] Max Planck Institute for Polymer Research, Ackermannweg 10, 55128 Mainz, Germany

ARTICLE INFO

Keywords:
Fano resonance
GHz acoustic phonons
Lamb waves
Brillouin light scattering
Nanomembranes

ABSTRACT

Observation of Fano resonances in various physical phenomena is usually ascribed to the coupling of discrete states with background continuum, as it has already been reported for various physical phenomena. Here, we report on Fano lineshapes of nonthermal GHz phonons generated and observed with pumped Brillouin light scattering in gold-silicon thin membranes, overlapping the broad zero-shift background of yet questionable origin. The system's broken mid-plane symmetry enabled the generation of coherent quasi-symmetric and quasi-antisymmetric Lamb acoustic waves/phonons, leading to the four orders-of-magnitude enhancement of Brillouin light scattering. Notably, the membrane asymmetry resulted also in the mode-dependent Stokes and anti-Stokes Fano lineshapes asymmetry.

Fano resonance theory is one of the most general models for describing resonance phenomena. Ugo Fano developed it in 1961 to explain asymmetric spectral lineshapes observed in the inelastic scattering of electrons by helium atoms [1], and his explanation was based on earlier work by Ettore Majorana [2]. Nevertheless, it can be applied to any phenomenon where discrete resonances energetically overlap and couple with a broad continuum of states. The shape of the Fano resonance curve depends on the phase of the oscillator and spans from the standard Lorentzian curve through a derivative-like shape to even anti-resonance (valley in the background signal). To date, numerous studies have reported Fano resonance lineshapes observed for various nanostructures (both synthetic and biological), showing interactions of charge carriers, plasmons, photons, and phonons [3–11]. Recently, the Fano lineshapes were captured by pumped Brillouin Light Scattering (pumped-BLS) for light inelastically scattered on nonthermal GHz phonons populated by femtosecond pulsed laser in ultrathin Si membranes [12]. Generally, sub-micrometer-thick membranes are an excellent platform for studying spatially confined acoustic phonons, called Lamb waves, spanning frequencies from sub-GHz to sub-THz regimes [13]. Investigation of such phonons can lead to a solution of analog preprocessing of high-frequency signals in long-range telecommunications and new GSM technologies, such as 5 G and 6 G [14]. Predictable enhancement and efficient detection of such signals, achieved by pumped-BLS, is a crucial step toward this technology's applicability [15].

In this work, we present experimental results of pumped-BLS performed on ultra-thin metal-semiconductor membranes. Our results reveal a generation of a discrete set of GHz nonthermal quasi-symmetric and quasi-antisymmetric acoustic Lamb waves (phonons) manifested as Fano lineshape peaks in the BLS spectra. Furthermore, the photogenerated phonons enhance the BLS signal by nearly four orders of magnitude compared to conventional spontaneous BLS. Notably, the broken mid-plane symmetry of the studied system leads to the unprecedented breaking of the Stokes-anti-Stokes lineshapes symmetry in BLS spectra and mode- (frequency-) dependent magnitude of Fano coupling.

Yet, the small scattering volume and poor light-induced heat dissipation of ultra-thin membranes limit the BLS signal vastly. At the same time, complicated carrier-lattice and anharmonic phonon-phonon interactions rapidly deplete the acoustic signals. To tackle these challenges, we recently developed a transducer-free, all-optical method, termed pumped-BLS, for generation, frequency- and momentum-resolved detection of nonthermal Lamb waves. We used pumped-BLS combining femtosecond laser excitation (λ_{pump}=780 nm, 150 fs pulses at 80 MHz repetition rate, 50x objective, NA=0.4) of GHz phonons with an inelastic light scattering of a continuous wave (CW) laser (λ_{probe}=532 nm, 20x objective, NA=0.4) – see Fig. 1 and Supplementary

* Corresponding author.
** Corresponding author at: Faculty of Physics, Adam Mickiewicz University, Poznań, ul. Uniwersytetu Poznańskiego 2, 61-614 Poznań, Poland.
E-mail addresses: rafal.bialek@amu.edu.pl (R. Białek), bartlomiej.graczykowski@amu.edu.pl (B. Graczykowski).

https://doi.org/10.1016/j.pacs.2023.100478
Received 19 December 2022; Received in revised form 21 March 2023; Accepted 21 March 2023
Available online 22 March 2023

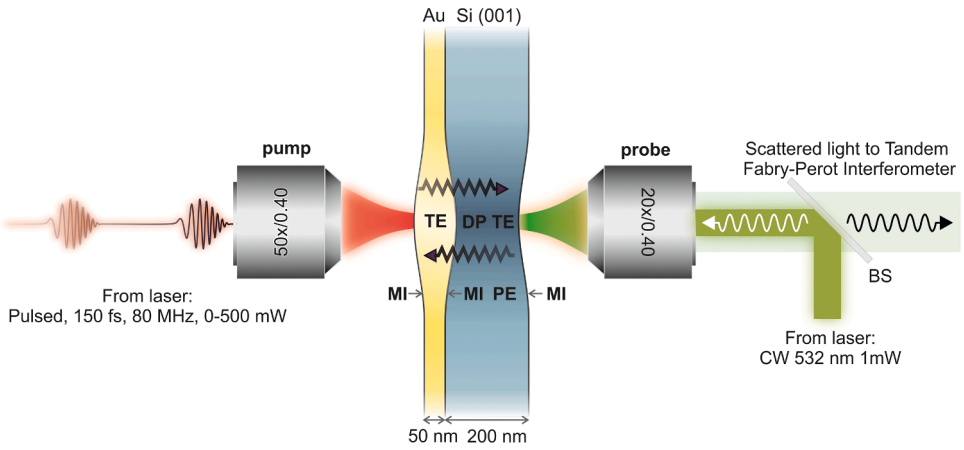

Fig. 1. Experimental system. Scheme of the pumped-BLS backscattering experiment in one of the measured configurations (pump on Au, probe on Si) with depicted mechanisms of scattering: moving interface (MI) and photoelastic effect (PE). The depicted expansion of the Au layer and contraction of Si layer are caused by the pump through thermal expansion (TE) and deformation potential (DP) mechanisms, respectively. BS – pellicle beam splitter.

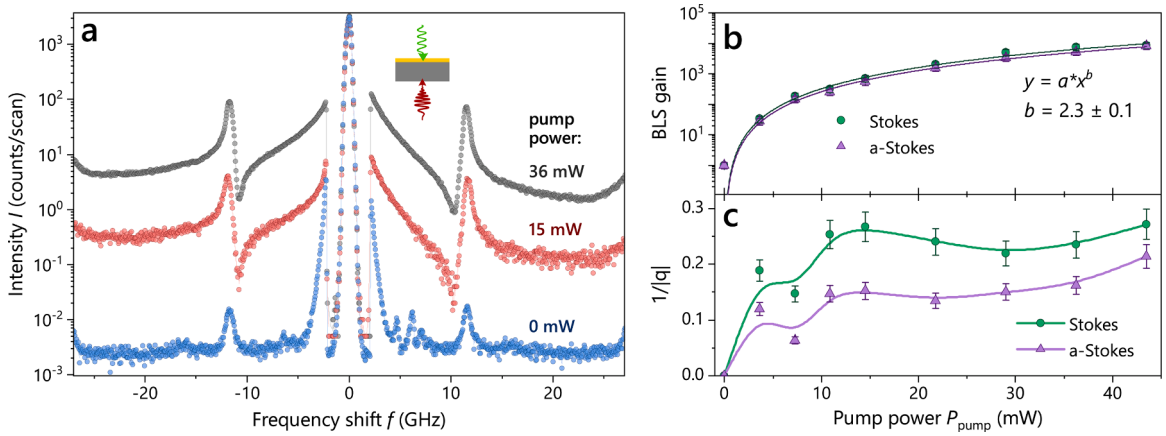

Fig. 2. BLS signal enhancement. (a) BLS spectra at fine free spectral range with the probe beam hitting at Au and pump beam at Si layer at exemplary pump powers. (b) BLS gain as a function of pump power calculated from the amplitude of single-Fano fit. Solid lines are fits with the power function. (c) Coupling efficiency as a function of the pump power. Solid lines are guides to the eye.

Material. The backscattering configuration at $\theta = 0^\circ$ was utilized, restricting all observed modes to standing waves. The nonthermal phonon excitation is based on the deformation potential (DP) mechanism and thermoelastic (TE) effect. At the same time, the inelastic light scattering detection originates in the moving interface (MI) and photoelastic (PE) effects [16,17], with the MI effect being the dominant contribution for nanostructures with plasmonic properties [18]. Here, we apply pumped-BLS on a bi-layer membrane made of 50 nm of Au sputtered on a single crystal (001) 200-nm thick Si membrane (AuSi MBs).

Fig. 2a displays the experimental pumped-BLS spectra obtained for the membrane pumped from the side of Si and probed from the side of Au layer using three exemplary powers of the pulsed laser. For the nonthermal spectra (15 and 36 mW), we can notice discrete spectroscopic peaks on top of a continuum of background excitations symmetric around zero BLS frequency shift. Those peaks can be assigned to the quasi-symmetric 1st-order Lamb wave (qS1), while their lineshapes can be represented as Fano resonances of the form:

$$I(f) = I_B(f)\frac{(q+\varepsilon)^2}{1+\varepsilon^2} \quad (1)$$

where: $I(f)$ – signal intensity at the frequency f, I_B – background intensity, q – Fano parameter defining peak asymmetry, ε – reduced energy, defined as $\varepsilon = (f - f_r)/(\Gamma/2)$, where f_r – resonant frequency, Γ – peak width parameter. The unpumped (thermal, 0 mW) spectrum reveals the low intensity and symmetric Stokes and anti-Stokes peaks (Fig. 2a, blue curve), while the peaks at lower frequencies are CW laser side bands. Switching on the pump leads to significant changes in the spectra (Fig. 2a, black and red curves). First, the signal is strongly enhanced at both the peaks and the background. Peak fitting with Eq. (1) yields a maximum BLS amplitude gain of about 8000 (see Supplementary Materials for fitting procedure). This significant BLS enhancement concerning our previous work on pristine Si membrane [12] can be attributed to the presence of the additional Au layer. Moreover, the dependence of the BLS gain on the pump power (Fig. 2b) is clearly nonlinear, with the exponent value 2.3 ± 0.1 suggesting multiphoton characteristics of the pumping process.

The observation of Fano lineshape is associated with the coupling between the continuum and discrete state. The magnitude of this coupling can be described as $1/|q|$ [12]. This value is shown in Fig. 2c and shows weak dependence on the pump power at a gain big enough so that the thermal phonon scattering is negligible.

The situation described above gets more complex for higher order Lamb modes and with varying the configuration of pump and probe. Fig. 3 gathers pumped-BLS spectra recorded for all four possible experimental geometries at the spectral range extended to 68 GHz. The observed peaks were identified based on the measured (thermal phonons) and calculated (finite element method, FEM) dispersion relations

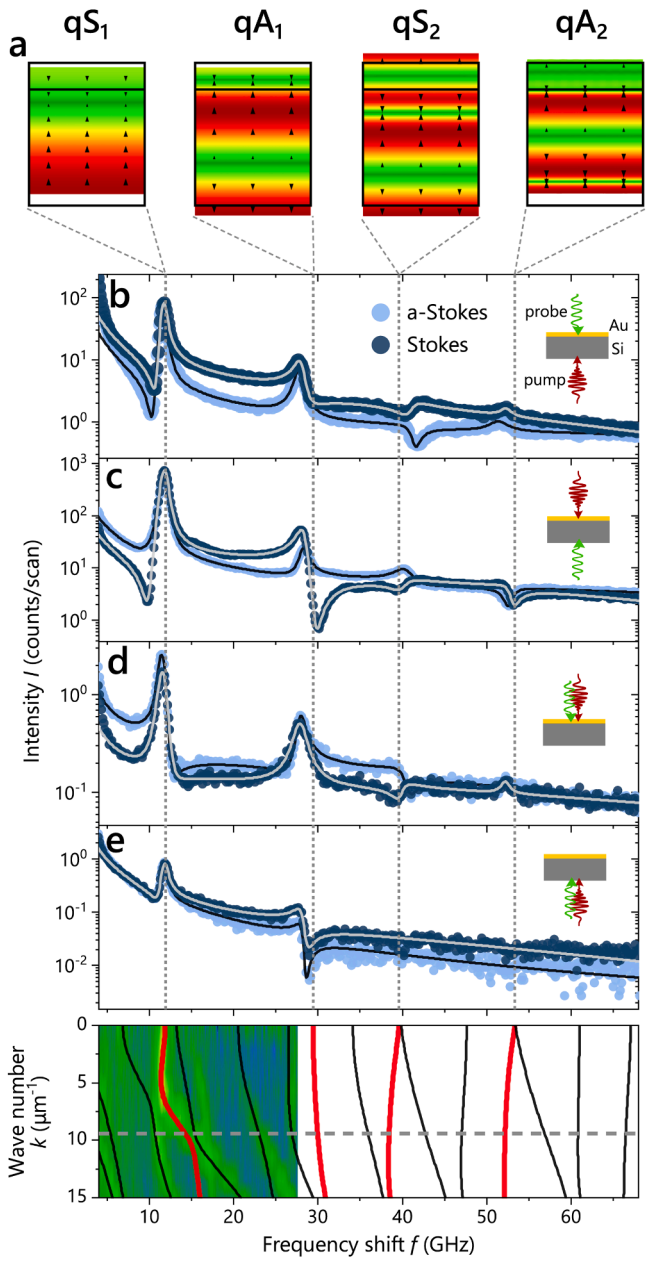

Fig. 3. Complexity of modes. (a) Displacement fields of four first observable Lamb modes as calculated by FEM, with quasi-symmetric (qS_n) and quasi-antisymmetric (qA_n) ones. Color scale: green – low, yellow – medium, red – large. (b-e) Overlayed Stokes and anti-Stokes branches of BLS spectra for different configurations of pump and probe (see notes in each panel). Solid lines are experimental data fits. (f) Experimental (colored map) and calculated (lines) thermal phonon dispersion of the studied sample. Red-line branches are active in the pumped-BLS experiment. The dashed horizontal line depicts a range of measured wavenumbers due to the probing objective lens NA.

plotted in Fig. 3f, as well as their calculated displacement fields (Fig. 3a).

The Fano lineshape spans over all peaks on the broader frequency range, and its extent varies with three different factors: Stokes/anti-Stokes side of the spectrum, frequency, and pump/probe configuration, evident in spectra presented in Fig. 3b-e. Note that Stokes parts of the spectra were mirrored horizontally for convenient comparison. Fitting of spectra by a sum of Fano peaks interfering with a background (see Supplementary Materials for details) proves that this variability is caused by the q factor, which can be attributed to the difference in the initial phase of the excited phonon $\varphi = \arctan(-1/q)$ [19]. Typically,

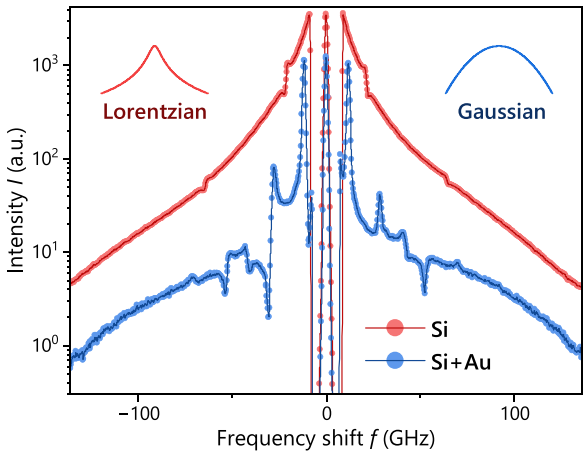

Fig. 4. Background signal lineshape. Comparison of lineshapes of BLS spectra taken for bare Si membrane and AuSi membrane at wide free spectral range. The inset shows shapes of theoretical Lorentzian and Gaussian functions in logarithmic scale for comparison.

spontaneous BLS spectra of thermal phonons are symmetric due to the low energy of oscillations in relation to the thermal energy. However, the asymmetry in amplitude has already been reported when the phonons are generated either by a thermal gradient [20] or are excited as coherent ones [12,16]. Nevertheless, the asymmetry of the shape of the peaks at Stokes and anti-Stokes sides presented here is an entirely new phenomenon. Furthermore, for the higher frequency modes, the peaks took even the shape of anti-resonance for specific configurations, a unique feature for BLS experiments, revealing a strong coupling of the discrete mode with the continuum.

The observations described above suggest that the probed phase, as extracted by the Fano coupling parameter, is affected by the phonon phase but also by the inelastic CW light scattering mechanisms. Notably, the phase of the scattered light is altered during reflection, and this phase shift depends on the refractive indices at the interface (Au, Si, or air). Moreover, which side is pumped affects the relative contribution of thermoelastic and deformation potential excitation and, thus, the phonon phase. Therefore, each geometry of pump-probe experiments is expected to give different Fano resonances.

An understanding of the background continuum signal is crucial for an accurate description of the observed Fano coupling. The shape of the background reported here for AuSi MB is significantly different from that reported earlier for bare Si membranes (Fig. 4) [12]. The background for the AuSi MB exhibits a Gaussian-like shape, while that for bare Si MB is Lorentzian-like. In the following, we will discuss a few possible sources of the background signal.

The background signal shape can be attributed to the Fourier transform of the scattering signal decay after each pump pulse. In more detail, the train of pulses generates a frequency comb in the BLS spectrum, albeit unresolvable, with employed spectral resolution and pump repetition rate (80 MHz) [21]. Thus, only the envelope of the comb given by the Fourier transform of individual pulse response is observable. For example, the exponentially decaying signal would lead to the Lorentzian background, whose width depends on the decay lifetime. Analogously, Gaussian decay would lead to the Gaussian background with a width dependency on the lifetime [22]. This interpretation is independent of the physical nature of the signal decay, which is yet to be determined.

The spectral shape of the background (Fig. 4), emerging from the way of sample relaxation from the state excited by a fs-laser pulse toward equilibrium, can reveal the transport properties of the (quasi) particles responsible for it. The theory of quasi-elastic scattering

described by Bern and Pecora associates the Lorentzian profile with diffusing species and the Gaussian profile with their ballistic movement [23]. In the case of bare Si MB, we have attributed the emergence of Fano resonances to the coupling of the Lamb waves with the photoexcited electron-hole plasma [12]. For a 50 mW power of 780 nm pulses focused on an area of 4.4 μm^2, the density of photogenerated carriers is estimated to be $\sim 10^{20}$ cm^{-3}, meaning that Si has transient optical properties very different than in equilibrium conditions. In comparison, the density of photogenerated carriers of a 260 nm thick Si membrane irradiated with a fluence of 12 mJ/cm^2 was estimated to be $3 \cdot 10^{19}$ cm^{-3}, while THz spectroscopy gave a slightly smaller value of $\sim 1.4 \cdot 10^{19}$ cm^{-3} [12]. The density of photogenerated carriers is difficult to estimate because it is affected by complicated processes like Auger recombination, carrier multiplication, and surface recombination, as well as carrier injection and multiphoton absorption in plasmonic-semiconducting heterostructures [24]. Photoexcited charges are known to produce a background in inelastic light scattering spectra [25]. In the case of a bare Si membrane, electron-hole pairs are generated in the whole volume of the semiconductor. Subsequently, charge carriers equilibrate with each other and with the lattice via electron-electron and electron-phonon interactions in the picosecond timescale [26]. The homogeneous excitation and the rapid thermalization cause charge carriers to diffuse randomly. This explains the Lorentzian shape of the background. In the case of the silicon-gold membrane, the situation is more complex. At the junction between gold (metal) and silicon (semiconductor), we have the formation of a Schottky barrier, causing band bending in silicon close to the interface and, thus, a potential gradient for excited charge carriers. Independently of the generation mechanism (multiphoton photoemission from gold or direct excitation of semiconductor through a band gap), the charge carrier movement is determined by the potential gradient. Therefore, their movement is ballistic, which can explain the Gaussian shape of the continuum background.

Yet, it is possible that the hot phonon gas created by electron-phonon coupling is also contributing to the continuum signal. Here, the unequal light absorption and electron-lattice thermalization timescales of Au and Si may cause interfacial phonon transport with ballistic characteristics, causing the Gaussian background [27]. Furthermore, the thermalization between charge carriers occurs in sub-picosecond timescales [28]. In contrast, the carrier-lattice thermalization time constant is in the order of 1 ps for Si nanomembranes [12] and ~4–5 ps for gold nanostructures and thin films [24,29].

Even though the conclusion on the source of the background signal cannot be drawn based on the obtained results, the most important fact is that this background is coupled with nonthermal phonons, manifesting both in substantial BLS gain and in a Fano lineshape. It lays a basis for further experiments on this system, such as momentum-resolved BLS to eradicate varying reflectance input, time-resolved BLS to explore time-evolution of background and peaks, use of dielectric-gold membranes to get rid of electron-hole pairs generation or switching towards bulk samples with gold layer to look for similar phenomena in surface or bulk waves.

Conclusively, for metal-semiconductor heterojunction, the fs laser excitation offers an unprecedented 8000-fold enhancement of the BLS signal (Fig. 2), with the previous record being a 300-fold enhancement for pure Si. Moreover, the symmetry lowering of AuSi MBs, compared to pure Si, enables the detection of multiple Lamb modes with both symmetric and antisymmetric character (Fig. 3). Moreover, we observed high variability of the coupling parameter depending on the pump and probe geometrical configuration, mode frequency and Stokes/anti-Stokes side of the spectrum. These findings prove that pumped BLS has strong potential for the characterization of phononic metamaterials, such as phononic crystals and topological phononics, especially in the presence of plasmonic components. These practical technical developments are accompanied by many intriguing observations that suggest exotic optomechanical interactions between ultrashort photon pulses, continuous wave light, and nonthermal coherent phonons. Future theoretical investigations will benefit from the detailed mapping of novel spectroscopic signatures concerning scattering geometry carried out in this work.

Declaration of Competing Interest

The authors declare the following financial interests/personal relationships which may be considered as potential competing interests: Bartlomiej Graczykowski reports financial support was provided by National Science Centre Poland. Rafal Bialek reports financial support was provided by National Science Centre Poland. Thomas Vasileiadis reports financial support was provided by National Science Centre Poland.

Data availability

Data will be made available on request.

Acknowledgments

We acknowledge Prof. Maciej Krawczyk for valuable discussions about the interpretation of the results of the project. This work was supported by National Science Centre Poland (UMO-2021/41/B/ST5/03038). TV acknowledges support from National Science Centre Poland (UMO-2021/43/D/ST3/02526).

Appendix A. Supplementary material

Supplementary data associated with this article can be found in the online version at doi:10.1016/j.pacs.2023.100478.

References

[1] U. Fano, Effects of configuration interaction on intensities and phase shifts, Phys. Rev. 124 (1961) 1866–1878, https://doi.org/10.1103/PhysRev.124.1866.
[2] E. Majorana, Teoria dei tripletti P' incompleti, Il Nuovo Cim. 8 (1931) 107–113.
[3] A.E. Miroshnichenko, S. Flach, Y.S. Kivshar, Fano resonances in nanoscale structures, Rev. Mod. Phys. 82 (2010) 2257–2298, https://doi.org/10.1103/RevModPhys.82.2257.
[4] A.C. Johnson, C.M. Marcus, M.P. Hanson, A.C. Gossard, Coulomb-modified Fano resonance in a one-lead quantum dot, Phys. Rev. Lett. 93 (2004), 106803, https://doi.org/10.1103/PHYSREVLETT.93.106803/FIGURES/4/MEDIUM.
[5] F. Hao, P. Nordlander, Y. Sonnefraud, P. van Dorpe, S.A. Maier, Tunability of subradiant dipolar and fano-type plasmon resonances in metallic ring/disk cavities: Implications for nanoscale optical sensing, ACS Nano 3 (2009) 643–652, https://doi.org/10.1021/NN900012R/ASSET/IMAGES/LARGE/NN-2009-00012R_0012.JPEG.
[6] M. Galli, S.L. Portalupi, M. Belotti, L.C. Andreani, L. O'Faolain, T.F. Krauss, Light scattering and Fano resonances in high-Q photonic crystal nanocavities, Appl. Phys. Lett. 94 (2009), 071101, https://doi.org/10.1063/1.3080683.
[7] S. Fan, J.D. Joannopoulos, Analysis of guided resonances in photonic crystal slabs, Phys. Rev. B 65 (2002), 235112, https://doi.org/10.1103/PhysRevB.65.235112.
[8] M. Kroner, A.O. Govorov, S. Remi, B. Biedermann, S. Seidl, A. Badolato, P. M. Petroff, W. Zhang, R. Barbour, B.D. Gerardot, R.J. Warburton, K. Karrai, The nonlinear Fano effect, 451 (2008) 311–7314, Nature 451 (2008) 7176, https://doi.org/10.1038/nature06506.
[9] H. Zhu, F. Yi, E. Cubukcu, Plasmonic metamaterial absorber for broadband manipulation of mechanical resonances, Nat. Photonics 10 (2016) 709–714, https://doi.org/10.1038/nphoton.2016.183.
[10] W. Zhang, T.J.A. Craddock, Y. Li, M. Swartzlander, R.R. Alfano, L. Shi, Fano resonance line shapes in the Raman spectra of tubulin and microtubules reveal quantum effects, Biophys. Rep. 2 (2022), 100043, https://doi.org/10.1016/j.bpr.2021.100043.
[11] R. Pant, S.S. A, A.B. Yelikar, Wideband excitation of Fano resonances and induced transparency by coherent interactions between Brillouin resonances, Sci. Rep. 8 (2018) 9175, https://doi.org/10.1038/s41598-018-27444-8.
[12] T. Vasileiadis, H. Zhang, H. Wang, M. Bonn, G. Fytas, B. Graczykowski, Frequency-domain study of nonthermal gigahertz phonons reveals Fano coupling to charge carriers, Sci. Adv. 6 (2020) eabd4540, https://doi.org/10.1126/sciadv.abd4540.
[13] M. Schubert, M. Grossmann, C. He, D. Brick, P. Scheel, O. Ristow, V. Gusev, T. Dekorsy, Generation and detection of gigahertz acoustic oscillations in thin membranes, Ultrasonics 56 (2015) 109–115, https://doi.org/10.1016/j.ultras.2014.06.018.
[14] W. Saad, M. Bennis, M. Chen, A vision of 6G wireless systems: applications, trends, technologies, and open research problems, IEEE Netw. 34 (2020) 134–142, https://doi.org/10.1109/MNET.001.1900287.

[15] R.C. Ng, A. el Sachat, F. Cespedes, M. Poblet, G. Madiot, J. Jaramillo-Fernandez, O. Florez, P. Xiao, M. Sledzinska, C.M. Sotomayor-Torres, E. Chavez-Angel, Excitation and detection of acoustic phonons in nanoscale systems, Nanoscale 14 (2022) 13428–13451, https://doi.org/10.1039/d2nr04100f.
[16] P. Ruello, V.E. Gusev, Physical mechanisms of coherent acoustic phonons generation by ultrafast laser action, Ultrasonics 56 (2015) 21–35, https://doi.org/10.1016/j.ultras.2014.06.004.
[17] B. Graczykowski, A. Gueddida, B. Djafari-Rouhani, H.-J. Butt, G. Fytas, Brillouin light scattering under one-dimensional confinement: symmetry and interference self-canceling, Phys. Rev. B 99 (2019), 165431, https://doi.org/10.1103/PhysRevB.99.165431.
[18] T. Vasileiadis, A. Noual, Y. Wang, B. Graczykowski, B. Djafari-Rouhani, S. Yang, G. Fytas, Optomechanical hot-spots in metallic nanorod-polymer nanocomposites, ACS Nano 16 (2022) 20419–20429, https://doi.org/10.1021/ACSNANO.2C06673/ASSET/IMAGES/LARGE/NN2C06673_0006.JPEG.
[19] O. v Misochko, M. v Lebedev, Fano interference at the excitation of coherent phonons: relation between the asymmetry parameter and the initial phase of coherent oscillations, J. Exp. Theor. Phys. 120 (2015) 651–663, https://doi.org/10.1134/S1063776115020168.
[20] D. Beysens, Y. Garrabos, G. Zalczer, Experimental evidence for brillouin asymmetry induced by a temperature gradient, Phys. Rev. Lett. 45 (1980) 403–406, https://doi.org/10.1103/PhysRevLett.45.403.
[21] A. Aleman, S. Muralidhar, A.A. Awad, J. Åkerman, D. Hanstorp, Frequency comb enhanced Brillouin microscopy, Opt. Express 28 (2020) 29540, https://doi.org/10.1364/oe.398619.
[22] M. Grossmann, M. Klingele, P. Scheel, O. Ristow, M. Hettich, C. He, R. Waitz, M. Schubert, A. Bruchhausen, V. Gusev, E. Scheer, T. Dekorsy, Femtosecond spectroscopy of acoustic frequency combs in the 100-GHz frequency range in Al/Si membranes, Phys. Rev. B Condens Matter Mater. Phys. 88 (2013) 1–9, https://doi.org/10.1103/PhysRevB.88.205202.
[23] B.J. Berne, R. Pecora, Dynamic Light Scattering, Dover Publications, Mineola, NY, 2000.
[24] T. Pincelli, T. Vasileiadis, S. Dong, S. Beaulieu, M. Dendzik, D. Zahn, S.E. Lee, H. Seiler, Y. Qi, R.P. Xian, J. Maklar, E. Coy, N.S. Mueller, Y. Okamura, S. Reich, M. Wolf, L. Rettig, R. Ernstorfer, Observation of multi-directional energy transfer in a hybrid plasmonic–excitonic nanostructure, Adv. Mater. 35 (2023), 2209100, https://doi.org/10.1002/ADMA.202209100.
[25] J. Huang, W. Wang, C.J. Murphy, D.G. Cahill, Resonant secondary light emission from plasmonic Au nanostructures at high electron temperatures created by pulsed-laser excitation, Proc. Natl. Acad. Sci. 111 (2014) 906–911, https://doi.org/10.1073/pnas.1311477111.
[26] M. Bernardi, D. Vigil-Fowler, J. Lischner, J.B. Neaton, S.G. Louie, Ab initio study of hot carriers in the first picosecond after sunlight absorption in silicon, Phys. Rev. Lett. 112 (2014), 257402, https://doi.org/10.1103/PHYSREVLETT.112.257402/FIGURES/4/MEDIUM.
[27] A. Koreeda, R. Takano, S. Saikan, Light scattering in a phonon gas, Phys. Rev. B Condens Matter Mater. Phys. 80 (2009) 1–25, https://doi.org/10.1103/PhysRevB.80.165104.
[28] M. Wörle, A.W. Holleitner, R. Kienberger, H. Iglev, Ultrafast hot-carrier relaxation in silicon monitored by phase-resolved transient absorption spectroscopy, Phys. Rev. B 104 (2021), L041201, https://doi.org/10.1103/PHYSREVB.104.L041201/FIGURES/5/MEDIUM.
[29] T. Vasileiadis, L. Waldecker, D. Foster, A. da Silva, D. Zahn, R. Bertoni, R. E. Palmer, R. Ernstorfer, Ultrafast heat flow in heterostructures of Au nanoclusters on thin films: Atomic disorder induced by hot electrons, ACS Nano 12 (2018) 7710–7720, https://doi.org/10.1021/ACSNANO.8B01423/ASSET/IMAGES/LARGE/NN-2018-01423R_0005.JPEG.

Rafał Białek obtained his PhD in physics in 2021 (Adam Mickiewicz University Poznań, Poland) for his work in the field of fundamental and application research on primary steps of photosynthesis, primarily in purple bacteria. He is currently employed as a post-doctoral researcher at Adam Mickiewicz University, Poznań, Poland working with Brillouin light scattering spectroscopy. His scientific interest comprise of both solid state physics of nanoscale materials and biophysics of photosynthetic apparatus in biohybrid solar devices. His basic tools are Brillouin light scattering spectroscopy, time-resolved absorption and emission spectroscopy and electrochemistry.

Thomas Vasileiadis studied physics (BSc) and materials science (MSc) in the University of Patras. During his master studies he worked as a research assistant in the Institute of Chemical Engineering Sciences ICEHT-FORTH. He then moved for his PhD studies in the group of Prof. Dr. Ralph Ernstorfer in the Fritz Haber Institute of the Max Planck Society. The topic of his thesis is 'Ultrafast energy flow and structural changes in nanoscale heterostructures'. He then joined the Faculty of Physics of the Adam Mickiewicz University with a Marie Skłodowska-Curie Action widening fellowship. His current scientific interests involve Brillouin light scattering of nanomaterials.

Mikołaj Pochylski obtained his PhD in Physics in 2007 (at the Faculty of Physics of Adam Mickiewicz University, Poznań, Poland) for his Brillouin Spectroscopy studies of relaxation phenomena in polymer solutions. Currently he holds an assistance professor position at this institution. His current research interests concerns structural and dynamical processes in soft matter systems, morphology and mechanics of thin polymeric and crystalline membranes, as well as biomedical imaging and image analysis. His basic tools are quasi-elastic and inelastic scattering techniques, polarymetry, optical spectroscopy and microscopy.

Bartłomiej Graczykowski obtained his PhD in Physics in 2012 (AMU, Poznan, Poland). He was appointed as a post-doctoral researcher at ICN2 Barcelona in Spain (2013–2016) and MPIP Mainz in Germany (A. von Humboldt Foundation fellowship, 2016–2017). Currently he is an assistant professor at the Faculty of Physics of Adam Mickiewicz University, Poznań, Poland and guest researcher at the Max Planck Institute for Polymer Research in Mainz, Germany. His research activities include advanced inelastic light scattering techniques (Brillouin, Raman) applied to nanostructures, hypersound and heat transport at the nanoscale in confined and organized systems.